Radiology

Marc Bazot, MD
Emile Darai, MD, PhD
Roula Hourani, MD
Isabelle Thomassin, MD
Annie Cortez, MD
Serge Uzan, MD
Jean-Noël Buy, MD

Index terms:
Bladder, diseases, 83.3192
Bladder, MR, 83.121411, 83.121412, 83.121415
Endometriosis, 75.318, 83.3192, 855.3192
Intestines, diseases, 758.318
Intestines, MR, 758.121411, 758.121412, 758.121415
Vagina, abnormalities, 855.3192

Published online before print
10.1148/radiol.2322030762
Radiology 2004; 232:379–389

Abbreviation:
USL = uterosacral ligament

[1] From the Departments of Radiology (M.B., R.H., I.T.), Pathology (A.C.), and Obstetrics and Gynecology (E.D., S.U.), Hôpital Tenon, Assistance Publique-Hôpitaux de Paris, 4 rue de la Chine, Paris 75020, France; and Department of Radiology, Hôtel Dieu de Paris, France (J.N.B.). Received May 20, 2003; revision requested July 31; final revision received November 14; accepted December 19. **Address correspondence to** M.B. (e-mail: *marc.bazot@tnn.ap-hop-paris.fr*).

Author contributions:
Guarantor of integrity of entire study, M.B.; study concepts, M.B., J.N.B., S.U.; study design, M.B., J.N.B., A.C.; literature research, R.H., I.T.; clinical studies, R.H., I.T.; data acquisition, R.H., I.T., A.C., S.U., E.D., J.N.B.; data analysis/interpretation, M.B., E.D., A.C., J.N.B.; statistical analysis, M.B.; manuscript preparation, M.B., E.D., R.H., I.T., J.N.B.; manuscript definition of intellectual content, M.B., J.N.B.; manuscript editing, M.B.; manuscript revision/review, M.B., E.D., J.N.B.; manuscript final version approval, all authors

Deep Pelvic Endometriosis: MR Imaging for Diagnosis and Prediction of Extension of Disease[1]

PURPOSE: To prospectively evaluate the accuracy of magnetic resonance (MR) imaging for the preoperative diagnosis of deep pelvic endometriosis and extension of the disease.

MATERIALS AND METHODS: One hundred ninety-five patients (mean age, 34.2 years; range, 20–71 years) who were suspected of having pelvic endometriosis were recruited at two institutions. Two experienced radiologists evaluated the MR images independently. Deep pelvic endometriosis was defined as implants or tissue masses that appeared as hypointense areas and/or hyperintense foci on T1- or T2-weighted MR images in the following locations: torus uterinus, uterosacral ligaments (USLs), vagina, rectovaginal septum, rectosigmoid, and bladder. MR imaging results were compared with surgical and pathologic findings. Sensitivity, specificity, predictive values, and accuracy of MR imaging for prediction of deep pelvic endometriosis were assessed.

RESULTS: Pelvic endometriosis was confirmed at pathologic examination in 163 (83.6%) of 195 patients. Endometriomas, peritoneal lesions, and deep pelvic endometriosis were diagnosed on the basis of surgical findings, alone or combined with pathologic findings, in 111 (68.1%), 83 (50.9%), and 103 (63.2%) of 163 patients, respectively. Torus uterinus and USL were the most frequent sites of deep pelvic endometriosis. The sensitivity, specificity, positive and negative predictive values, and accuracy of MR imaging for deep pelvic endometriosis were 90.3% (93 of 103), 91% (84 of 92), 92.1% (93 of 101), 89% (84 of 94), and 90.8% (177 of 195), respectively. The sensitivity, specificity, and accuracy, respectively, of MR imaging for the diagnosis of endometriosis in specific sites were as follows: USL, 76% (57 of 75), 83.3% (100 of 120), and 80.5% (157 of 195); vagina, 76% (16 of 21), 95.4% (166 of 174), and 93.3% (182 of 195); rectovaginal septum, 80% (eight of 10), 97.8% (181 of 185), and 96.9% (189 of 195); rectosigmoid, 88% (53 of 60), 97.8% (132 of 135), and 94.9% (185 of 195); and bladder, 88% (14 of 16), 98.9% (177 of 179), and 97.9% (191 of 195).

CONCLUSION: MR imaging demonstrates high accuracy in prediction of deep pelvic endometriosis in specific locations.

Endometriosis is defined as the presence of endometrial tissue outside the endometrium and the myometrium (1). The most common locations of endometriosis are the ovaries and the pelvic peritoneum, followed in order of decreasing frequency by deep lesions of the pelvic subperitoneal space (2, pp 394–398), the intestinal system, and the urinary system. Deep pelvic endometriosis, also called deep infiltrating endometriosis, is defined as infiltration of the implant of endometriosis under the surface of the peritoneum (3). Although peritoneal endometriosis can be asymptomatic, deep pelvic endometriosis is a cause of pelvic pain, dysmenorrhea, dyspareunia, dyschezia, and urinary symptoms and is associated with infertility. The histologic findings of deep pelvic endometriosis are mainly

characterized by fibromuscular hyperplasia that surrounds foci of endometriosis, and the foci sometimes contain small cavities (3).

Physical examination and laparoscopic exploration may not allow diagnosis or prediction of the extension of deep pelvic endometriosis, especially in pelvic subperitoneal sites (4). Transvaginal sonography is recommended for the diagnosis of endometriomas (5,6) and endometriosis of the bladder (7), but its value for the assessment of superficial peritoneal lesions, ovarian foci, and deep pelvic endometriosis is uncertain. Rectal endoscopic sonography with high-frequency probes (7.5–12 MHz) has been recommended for detection of endometriosis in rectal, rectovaginal, uterosacral, and/or rectosigmoid locations (8,9), but high-frequency sonography shows poor penetration. Magnetic resonance (MR) imaging is now commonly used for diagnosis of endometriomas, but its value for diagnosis of endometriosis in the bladder, in superficial peritoneal lesions, and in ovarian foci is controversial (7,10–12). MR imaging was recently used for the diagnosis of endometriosis in the uterosacral ligaments (USLs) but was found to lack sensitivity for diagnosis of the disease with rectal involvement (13).

The purpose of our study was to prospectively evaluate the accuracy of MR imaging for the preoperative diagnosis of deep pelvic endometriosis and extension of the disease.

MATERIALS AND METHODS

One hundred ninety-five patients (mean age, 34.2 years; range, 20–71 years) who were suspected of having pelvic endometriosis were recruited at two institutions from January 1998 to May 2002. The inclusion criteria were clinical symptoms (pelvic pain, infertility, nodules, or tenderness at physical examination) and/or sonographic signs (cysts with diffuse low-level internal echoes, multilocularity, or hyperechoic wall foci; abnormal linear thickening, nodules, or masses in specific subperitoneal locations) of endometriosis. All patients met the inclusion criteria, and they underwent MR imaging preoperatively for assessment of the value of this technique for the diagnosis of deep pelvic endometriosis and for the prediction of extension of the disease. In our study, the protocol was approved by local institutional review boards, and all patients provided informed consent.

MR Imaging Technique and Image Analysis

MR images were acquired with a 1- or 1.5-T MR imaging device (Harmony or Magnetom Vision; Siemens, Erlangen, Germany) with 5-mm-thick sections and a 1-mm gap, a rectangular field of view of 280 × 245 mm, and a matrix of 224 × 512 pixels. The protocol always included sagittal and transverse fast spin-echo T2-weighted MR imaging, transverse spin-echo or gradient-echo T1-weighted MR imaging with and without fat suppression, and transverse spin-echo or gradient-echo T1-weighted MR imaging with or without fat suppression after intravenous injection of 0.2 mL per kilogram body weight gadoterate meglumine (Dotarem; Guerbet, Aulnay-sous-Bois, France). The fast spin-echo T2-weighted sequence was performed with the following imaging parameters: repetition time msec/echo time msec, 4,500/128 (effective); echo train length, 23; and number of signals acquired, two. T1-weighted spin-echo sequences were performed with 600/15 and two signals acquired. Fast low-angle shot sequences were performed with and without fat saturation to obtain T1 contrast with a breath hold of 13 msec and the following parameters: 100/13, flip angle of 65°, and one signal acquired.

All sequences were performed with anterior and posterior saturation bands placed anteriorly and posteriorly to eliminate the high signal from the subcutaneous fat. Additional sequences were performed according to the location of abnormalities. After a rectal enema, the true fast imaging with steady-state precession sequence was performed in the sagittal and transverse planes with the following parameters: 6.3/3; flip angle, 70°; section thickness, 5 mm; rectangular field of view, 320 × 240 mm; and matrix, 256 × 198.

One hundred twenty-six (64.6%) of 195 patients received 10 mg of an antispasmodic drug (tiemonium methylsulphate, Visceralgine; Organon, Livron, France) intravenously at the onset of the examination to decrease peristalsis.

We made no attempt to analyze the accuracy of the pulse sequences individually. We did not quantitatively evaluate the usefulness of gadolinium-based contrast material for the diagnosis of deep pelvic endometriosis.

The MR images were analyzed prospectively by two radiologists (M.B., J.N.B.), one at each of our institutions, who each had more than 10 years of gynecologic imaging experience. The radiologists were blinded to clinical and sonographic findings, and each independently interpreted the images acquired at the other radiologist's institution. They were asked to determine whether endometriosis was present in the ovaries, according to previously described criteria (11,14), and in the superficial peritoneum at specific locations such as the ovarian fossa, uterine serosa, peritoneum of broad ligaments, Douglas pouch, and vesicouterine pouch, according to criteria of Ha et al (15) for diagnosis of hemorrhagic implants. They also were asked to identify deep pelvic endometriosis, which was defined as the presence of implants of endometriosis under the peritoneum, in the anatomic subperitoneal space, and in other intraperitoneal structures (mainly the intestinal tract and especially the sigmoid colon); to describe the topography of the uterus (anteflexed or retroflexed); and to identify adenomyosis, according to previously described criteria (16,17).

Analysis of Deep Pelvic Endometriosis

The diagnosis of deep pelvic endometriosis was based on the joint presence of signal intensity abnormalities (18) and morphologic abnormalities.

Signal intensity abnormalities.—Signal intensity abnormalities were observed as hyperintense foci that corresponded to hemorrhagic foci on T1-weighted and/or fat-suppressed T1-weighted MR images. Other abnormalities included small hyperintense cavities observed on T2-weighted MR images. Still other irregularities included tissue areas that corresponded to fibrosis, with signal intensity close to that of pelvic muscle on T1- and T2-weighted MR images. These latter irregularities were observed with or without foci or cavities and with or without contrast enhancement after gadolinium-based contrast material injection.

Morphologic abnormalities.—Morphologic abnormalities with regular or irregular stellate margins were evaluated at each site of posterior or anterior deep pelvic endometriosis. The abnormalities varied according to the anatomic location as follows: posterior compartment, anterior compartment, intestinal tract involvement, and frozen pelvis.

Abnormalities of the posterior compartment were recorded. Among these abnormalities was torus uterinus, which was the presence of a mass or thickening in the upper middle portion of the posterior cervix. Torus uterinus is anatomically defined by the presence of a small transverse thickening that binds the orig-

inal insertion of USLs on the posterior wall of the uterus (2, p 370).

Another abnormality, involvement of a USL with endometriosis, was recorded when the ligament bore a nodule with regular or stellate margins or showed fibrotic thickening with regular or irregular margins compared with the margins of the contralateral USL. The unilateral or bilateral nature of the involvement and involvement of the torus uterinus (arciform abnormality) were noted. When a USL was considered abnormal and was clearly distinguished from adjacent structures, the size of its proximal portion, close to insertion on the cervix, was measured on the transverse or sagittal view.

Abnormalities of the vagina and/or cervix were observed as obliteration of the hypointense signal of the posterior vaginal wall on T2-weighted MR images, with thickening or a mass that contained or did not contain foci behind the posterior wall of the cervix.

Abnormalities of the anterior wall of the rectum and the sigmoid colon were observed as disappearance of the fat tissue plane lying between the uterus and the rectum and sigmoid colon, disappearance of the hypointense signal of the anterior wall of the rectum and sigmoid colon on T2-weighted MR images, and presence of a tissue mass extending on the anterior wall of the rectum and the inferior wall of the sigmoid colon showing contrast enhancement on T1-weighted MR images. Abnormalities that formed an obtuse angle with the wall of the rectum and sigmoid colon, the degree of extension, and particularly the distance between the lower limit of the fibrotic mass and the rectal-anal junction were recorded. The presence or absence of associated endometriosis on the posterior wall of the uterus, in continuity with deep pelvic lesions of endometriosis, was noted.

Abnormalities of the pouch of Douglas were observed as partial or complete obliteration with presence or absence of suspended or lateralized fluid collection.

An abnormality of the rectovaginal septum was observed as a nodule or mass that passed through the lower border of the posterior lip of the cervix (under the peritoneum).

Abnormalities of the anterior compartment included bladder involvement and a vesicouterine block of tissue. With bladder involvement, a nodule or mass usually was located at the level of the vesicouterine pouch and formed an obtuse angle with the bladder wall, extended through the bladder wall and involved the muscularis layer (obliteration of the hypointense signal of the wall on T2-weighted MR images), or protruded into the lumen with invasion of the mucosal layer. A vesicouterine block of tissue was associated with diffuse anterior endometriosis and complete obstruction of the vesicouterine pouch.

Intestinal tract involvement included abnormalities observed at intraperitoneal locations such as the sigmoid colon, the lower part of the sigmoid colon with rectal involvement and with or without adhesions to the posterior wall of the uterine body, and the presence of posterior wall endometriosis.

Frozen pelvis is an abnormality that corresponds to extension of endometriosis to multiple adjacent pelvic structures. With this abnormality, a block of tissue is created that simulates carcinoma and is not amenable to complete surgical resection.

Surgical and Pathologic Findings

One hundred thirty-six patients underwent laparoscopy and 59 underwent laparotomy with (n = 20) or without (n = 39) initial diagnostic laparoscopy.

Deep pelvic endometriosis was diagnosed in one of the following isolated or associated circumstances: In the first circumstance, endometrial tissue (endometrial gland and stroma) was found at histopathologic examination of at least one resected subperitoneal lesion (3). In the second circumstance, direct visualization of a deep pelvic lesion of endometriosis was possible at laparoscopy or laparotomy, associated with only fibrosis at biopsy, or without biopsy of the deep lesion (19). In this case, subperitoneal endometriosis was diagnosed on the basis of the presence of another histologically proved location of endometriosis. In the third circumstance, complete cul-de-sac obliteration secondary to endometriosis was observed. The tissue that caused the obliteration was unresectable because the surgeons considered it too risky or because the patient refused to undergo surgery. In accordance with Reich et al (20), we considered that deep retrocervical endometriosis was present under the peritoneum in such cases.

Statistical Analysis

Eighty-five patients had deep pelvic endometriosis that was confirmed at surgery, and these results provided an expected a priori sensitivity of 85% and a statistical power of 80%. Thus, we were able to achieve a precision of 1.0 with 95% CI for sensitivity of 70%. We expected a prevalence of approximately 50%, with allowance of a similar precision for specificity. Therefore, we designed our study with a sample of about 200 patients.

The sensitivity, specificity, positive and negative predictive values, and accuracy of MR imaging were evaluated for ovarian and peritoneal involvement and for each site of deep pelvic endometriosis.

RESULTS

Surgical and Pathologic Findings

In 163 (83.6%) of 195 patients, pelvic endometriosis was confirmed at surgery and was found in at least one location (ovary, peritoneum, or subperitoneal space) at pathologic examination. Among 163 patients with proved pelvic endometriosis, endometriomas (111 [68.1%]), superficial peritoneal implants (83 [50.9%]), and deep pelvic endometriosis (103 [63.2%]) were found at surgery alone or at surgery and biopsy. The location of deep pelvic endometriosis is reported in Table 1. In 103 patients, deep pelvic endometriosis involvement was as follows: posterior compartment, 97 (94.2%) patients; anterior compartment, 16 (15.5%) patients; both compartments, 10 (9.7%) patients. Thirty-two (19.6%) of 163 patients with proved pelvic endometriosis had isolated deep pelvic endometriosis without peritoneal or ovarian involvement.

Among 32 patients without proved pelvic endometriosis, findings were as follows: normal examination (n = 13), hydrosalpinx (n = 5), functional ovarian cyst (n = 4), serous ovarian tumor (n = 3), subserous leiomyoma (n = 3), ovarian fibroma (n = 2), and dermoid cyst (n = 2).

MR Imaging Results

Overall diagnostic performance of MR imaging for deep pelvic endometriosis was evaluated with respect to the correlation between MR imaging results and surgical findings alone and the correlation between MR imaging results and surgical and pathologic findings.

Tissue areas that corresponded to fibrosis on MR images were present in all patients with proved deep pelvic endometriosis. Hyperintense foci on T1-weighted and/or fat-suppressed T1-weighted MR images that corresponded to hemorrhagic foci or small hyperintense cavities on T2-weighted MR images that corresponded to cystic foci at pathologic ex-

amination were present in 59 (61%) of 97 patients with posterior deep pelvic endometriosis and in 16 (100%) of 16 patients with endometriosis in the bladder. Among 10 patients with false-negative MR imaging results, endometriosis was found in the USL in nine and in the torus uterinus in four at surgery. Among eight patients with false-positive MR imaging results, endometriosis was diagnosed in the USL in seven and in the torus uterinus in two at MR imaging. The sensitivity, specificity, positive and negative predictive values, and accuracy of MR imaging for deep pelvic endometriosis were 90.3% (93 of 103), 91% (84 of 92), 92.1% (93 of 101), 89% (84 of 94), and 90.8% (177 of 195), respectively (Table 2).

TABLE 1
Location of Deep Pelvic Endometriosis Diagnosed at Surgery and Confirmed at Histologic Examination

Subperitoneal Location (n = 103)	Diagnosis at Surgery	Surgical Specimen	Confirmation at Pathologic Examination
Posterior compartment	97	78	70
Torus uterinus	68	NA	NA
USL	75	56	51
Torus uterinus or USL	89	NA	NA
Vagina	21	17	15
Intestine	60	39	38
Sigmoid colon	8	6	6
Rectosigmoid junction	39	24	23
Rectum	10	9	9
Rectovaginal septum	10	10	10
Obliteration of pouch of Douglas			
Complete	55	NA	NA
Partial	14	NA	NA
Anterior compartment	16	15	15
Bladder, isolated	6	6	6
Bladder, associated with deep posterior pelvic endometriosis	10	9	9

Note.—Data are numbers of patients. NA = not available.

TABLE 2
Deep Pelvic Endometriosis: Correlation between MR Imaging Results and Surgical and Pathologic Findings

MR Imaging Results	Positive Surgical and Pathologic Findings	Negative Surgical and Pathologic Findings	No. of Patients
Positive	93	8	101
Negative	10	84	94
Total	103	92	195

Note.—Positive indicates that endometriosis was present, and negative indicates that it was not. Sensitivity was 90.3%; specificity, 91%; positive predictive value, 92.1%; negative predictive value, 89%; and accuracy, 90.8%.

TABLE 3
USL Involvement: Correlation between MR Imaging Results and Surgical Findings

MR Imaging Results	Positive Surgical Findings	Negative Surgical Findings	No. of Patients
Positive	57	20	77
Negative	18	100	118
Total	75	120	195

Note.—Positive indicates that USL involvement was present, and negative indicates that it was not. Sensitivity was 76%; specificity, 83.3%; positive predictive value, 74%; negative predictive value, 84.7%; and accuracy, 80.5%.

MR Imaging Results and Location of Endometriosis

USL and torus uterinus.—Evaluation of USL involvement with respect to the correlation between MR imaging results and surgical findings is described in Table 3. Unilateral or bilateral USL involvement was present in 30 and 45 patients, respectively (Fig 1). The size of the involved USL was between 4 and 20 mm (mean, 11.2 mm) (Figs 2, 3). Among 18 patients with false-negative MR imaging results, a retroflexed uterus masked the origin of the USL in six, the endometrioma lay on the USL in six, and the bowel was juxtaposed to the USL in two; misinterpretation occurred in four. In 20 patients, MR imaging results were false-positive: in five, clear delineation from the endometrioma that lay on the USL was difficult; in seven, adhesions hid the USL; in eight, measurement of and assessment of regularity of the USL were difficult. Among these 20 patients, eight had frozen pelvis at surgery. The sensitivity, specificity, positive and negative predictive values, and accuracy of MR imaging for the diagnosis of USL involvement compared with surgical findings were 76% (57 of 75), 83.3% (100 of 120), 74% (57 of 77), 84.7% (100 of 118), and 80.5% (157 of 195), respectively (Table 3).

Pathologic analysis was performed. Among 75 patients with surgically proved involvement, the lesions were resected in 56. Pathologic findings were positive for disease in 51 of 56 patients. Only fibrosis was indicated in the other five cases.

Correlation between the pathologic findings and the MR imaging results that pertain to USL involvement is described in Table 4. Among seven patients with false-negative MR imaging results, a retroflexed uterus masked the origin of the USL in four, the endometrioma lay on the USL in four, and the bowel was juxtaposed to the USL in one. Thirty-three patients had false-positive MR imaging results: in eight, the endometrioma masked the USL; in nine, adhesions masked the USL; in eight, measurement of and assessment of the regularity of the USL were difficult; and in eight, frozen pelvis was diagnosed. The sensitivity, specificity, positive and negative predictive values, and accuracy of MR imaging for the diagnosis of USL involvement compared with pathologic findings were 86% (44 of 51), 77.1% (111 of 144), 57% (44 of 77), 94.1% (111 of 118), and 79.5% (155 of 195), respectively.

Torus uterinus involvement was mainly

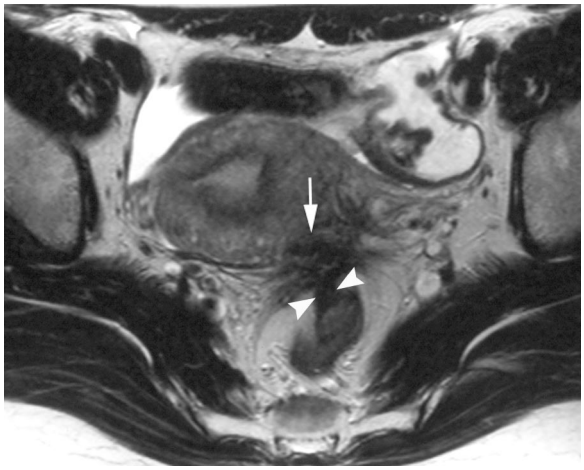

Figure 1. Transverse T2-weighted fast spin-echo MR image (4,500/128) demonstrates irregular tissue area (related to fibrosis), with signal intensity close to that of pelvic muscle in the torus uterinus and USLs, that forms an arciform abnormality (arrow). Thickening of anterior rectal wall, which forms obtuse angle with normal wall, suggests rectal wall involvement (arrowheads); this involvement was confirmed at surgery. True-positive diagnosis of torus uterinus and bilateral USL involvement with endometriosis, along with rectal involvement, was determined at MR imaging.

Figure 3. Transverse T2-weighted fast spin-echo MR image (4,500/128) demonstrates regular linear thickening of the right USL (thick arrow). Adipose tissue plane lying between uterus and rectum aids in ruling out intestinal involvement (thin arrow). True-positive diagnosis of linear uterosacral involvement with endometriosis was determined at MR imaging.

Figure 2. Sagittal T2-weighted fast spin-echo MR image (4,500/128) demonstrates irregular USL nodule (thin arrow) adjacent to posterior endometriosis of the uterus, large endometrioma, multiple uterine leiomyomas (thick arrow), and nabothian cyst in the cervical region. True-positive diagnosis of nodular USL involvement with endometriosis was determined at MR imaging.

determined on the basis of surgical findings. This involvement was associated with unilateral or bilateral USL involvement in 54 patients. Involvement of the torus uterinus or USL was detected in 89 (86.4%) of 103 patients at surgery and in 74 (83%) of 89 patients at MR imaging.

Vagina.—Correlation between surgical findings and MR imaging results for vaginal involvement is described in Table 5. All five patients with false-negative results at MR imaging had positive results at retrospective analysis. The eight patients with false-positive MR imaging results had a retroflexed uterus ($n = 5$), a frozen pelvis ($n = 2$), or both ($n = 1$). The sensitivity, specificity, positive and negative predictive values, and accuracy of MR imaging for the diagnosis of vaginal involvement compared with surgical findings were 76% (16 of 21), 95.4% (166 of 174), 67% (16 of 24), 97.1% (166 of 171), and 93.3% (182 of 195), respectively.

Pathologic analysis was performed. Seventeen of 21 patients with surgically proved involvement underwent biopsy. Biopsy results in 15 patients were positive. In two patients, biopsy specimens did not correspond to vaginal tissue.

Correlation between pathologic findings and MR imaging results for vaginal involvement is described in Table 6. Although there were three false-negative cases at the prospective MR imaging study, a retrospective analysis of MR images helped in the correct diagnosis of this extension. Among 12 patients with false-positive results, biopsy was not performed in four and rectovaginal septum involvement was diagnosed in four. Six patients had a retroflexed uterus, and one had frozen pelvis. The sensitivity, specificity, positive and negative predictive values, and accuracy of MR imaging for the diagnosis of vaginal involvement compared with pathologic findings were 80% (12 of 15), 93.3% (168 of 180), 50%

(12 of 24), 98.2% (168 of 171), and 92.3% (180 of 195), respectively.

Rectovaginal septum.—Correlation between surgical and pathologic findings and MR imaging results was evaluated. All lesions of the rectovaginal septum that were found during surgery were resected. Lesions at this site of involvement were always accompanied by lesions of endometriosis at other posterior locations, such as USL (n = 10), vagina (n = 7), or rectosigmoid (n = 10) (Fig 4). Rectovaginal septum involvement is described in Table 7. Posterior deep pelvic endometriosis was diagnosed at MR imaging in two patients with MR imaging results that were false-negative for rectovaginal involvement. Discrepancies between MR imaging and surgical findings were noted in regard to the precise anatomic location. The four false-positive results were observed in three patients with frozen pelvis (resection was not performed in two patients) and one patient in whom the precise extension of posterior involvement with endometriosis that was predicted with MR imaging differed from that seen during surgery. The sensitivity, specificity, positive and negative predictive values, and accuracy of MR imaging for the diagnosis of rectovaginal septum involvement compared with pathologic findings were 80% (eight of 10), 97.8% (181 of 185), 67% (eight of 12), 98.9% (181 of 183), and 96.9% (189 of 195), respectively.

Intestine.—Correlation between surgical findings and MR imaging results was evaluated. MR imaging results for intestinal involvement in the 60 patients with surgically proved involvement are reported in Table 8. Among seven patients with false-negative MR imaging results, six had involvement limited to the serosa at MR imaging and one had rectal involvement that was overlooked. No intestinal abnormalities were noted during surgical exploration in three patients with false-positive MR imaging results. The sensitivity, specificity, positive and negative predictive values, and accuracy of MR imaging for the diagnosis of intestinal involvement compared with surgical findings were 88% (53 of 60), 97.8% (132 of 135), 95% (53 of 56), 95.0% (132 of 139), and 94.9% (185 of 195), respectively.

Three MR imaging patterns were observed according to the site of the lesions. The most frequent location was the rectosigmoid junction (n = 39). In most cases the rectum was attracted forward, converged on the torus uterinus, and obliterated the cul-de-sac associated with USL involvement. Fluid was sometimes visualized lateral to the rectum or hanging above the fibrotic area. The lesion itself was visualized as a thickening of the rectal wall and formed an obtuse angle with the normal wall. On transverse T2-weighted MR images, the lesion of the anterior wall of the rectum was usually located between the 10- and 2-o'clock positions; it yielded a triangular aspect, with the tip of the triangle pointing anteriorly. The aspect of the lesion was mainly fibromuscular and sometimes contained hyperintense foci on T1-weighted or fat-suppressed MR images. Gadolinium-based contrast material injection was used to prevent a false-positive diagnosis of rectal wall invasion, and it helped the radiologist to clearly distinguish between the lesion and the rectal wall.

In eight patients, the intestinal involvement was restricted to the sigmoid colon. The involvement was always located on the lower surface of the colon. Involvement at these locations was difficult to diagnose with standard MR imaging sequences. Opacification with a water enema was very helpful in the confirmation of this diagnosis in two patients (Fig 5).

In 10 patients, the lesion involved the lower part of the pouch of Douglas, and it extended downward to the anterolateral wall of the rectum and to the rectovaginal septum. In rectal locations, the distance between the lower border of the fibrotic mass and the junction of the pelvic and perineal rectum could be accu-

TABLE 4
USL Involvement: Correlation between MR Imaging Results and Pathologic Findings

MR Imaging Results	Positive Pathologic Findings	Negative Pathologic Findings	No. of Patients
Positive	44	33	77
Negative	7	111	118
Total	51	144	195

Note.—Positive indicates that USL involvement was present, and negative indicates that it was not. Sensitivity was 86%; specificity, 77.1%; positive predictive value, 57%; negative predictive value, 94.1%; and accuracy, 79.5%.

TABLE 5
Vaginal Involvement: Correlation between MR Imaging Results and Surgical Findings

MR Imaging Results	Positive Surgical Findings	Negative Surgical Findings	No. of Patients
Positive	16	8	24
Negative	5	166	171
Total	21	174	195

Note.—Positive indicates that vaginal involvement was present, and negative indicates that it was not. Sensitivity was 76%; specificity, 95.4%; positive predictive value, 67%; negative predictive value, 97.1%; and accuracy, 93.3%.

TABLE 6
Vaginal Involvement: Correlation between MR Imaging Results and Pathologic Findings

MR Imaging Results	Positive Pathologic Findings	Negative Pathologic Findings	No. of Patients
Positive	12	12	24
Negative	3	168	171
Total	15	180	195

Note.—Positive indicates that vaginal involvement was present, and negative indicates that it was not. Sensitivity was 80%; specificity, 93.3%; positive predictive value, 50%; negative predictive value, 98.2%; and accuracy, 92.3%.

TABLE 7
Rectovaginal Septum Involvement: Correlation between MR Imaging Results and Surgical and Pathologic Findings

MR Imaging Results	Positive Surgical and Pathologic Findings	Negative Surgical and Pathologic Findings	No. of Patients
Positive	8	4	12
Negative	2	181	183
Total	10	185	195

Note.—Positive indicates that rectovaginal septum involvement was present, and negative indicates that it was not. Sensitivity was 80%; specificity, 97.8%; positive predictive value, 67%; negative predictive value, 98.9%; and accuracy, 96.9%.

TABLE 8
Intestinal Involvement: Correlation between MR Imaging Results and Surgical Findings

MR Imaging Results	Positive Surgical Findings	Negative Surgical Findings	No. of Patients
Positive	53	3	56
Negative	7	132	139
Total	60	135	195

Note.—Positive indicates that intestinal involvement was present, and negative indicates that it was not. Sensitivity was 88%; specificity, 97.8%; positive predictive value, 95%; negative predictive value, 95.0%; and accuracy, 94.9%.

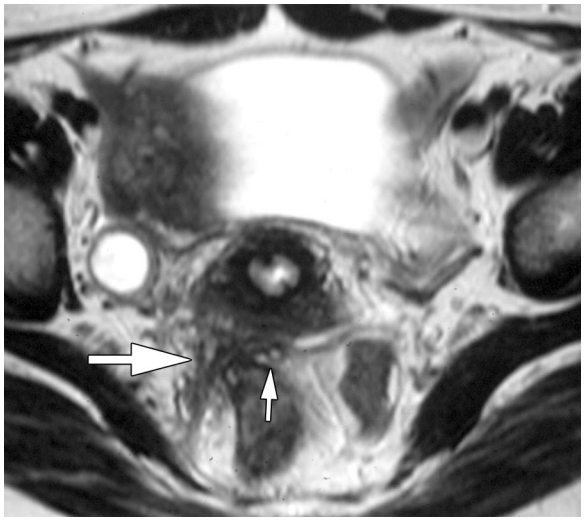

Figure 4. Transverse T2-weighted fast spin-echo MR image (4,500/128) demonstrates irregular solid area with signal intensity close to that of pelvic muscle (thick arrow) at patient's right; area contains foci of high signal intensity (thin arrow) between lateral part of rectovaginal septum and rectal wall. True-positive diagnosis of rectovaginal involvement with endometriosis was determined at MR imaging.

rately evaluated and was between 30 and 70 mm (mean, 49 mm).

Correlation between pathologic findings and MR imaging results was evaluated. Resection was performed in 39 of 60 patients with surgically proved involvement. Thirty-eight patients had endometrial foci, fibrosis, and muscular hyperplasia of the muscularis propria at pathologic examination. One patient had only fibrosis of the muscularis propria. MR imaging results and pathologic findings for intestinal involvement are compared in Table 9. In two patients with false-negative results, one patient had rectal involvement that was visible retrospectively. There were no false-positive results. The sensitivity, specificity, positive and negative predictive values, and accuracy of MR imaging for the diagnosis of intestinal involvement compared with pathologic findings were 95% (37 of 39), 100% (156 of 156), 100% (37 of 37), 98.7% (156 of 158), and 99.0% (193 of 195), respectively.

Bladder.—Correlation between surgical and pathologic findings and MR imaging results was evaluated. Among 16 patients with surgically proved bladder involvement, 15 had bladder lesions that were resected; all were positive for disease at pathologic examination (Fig 6). The results for bladder involvement are reported in Table 10. In two patients with false-negative results, MR imaging failed to show the extension of vesicouterine pouch involvement through the bladder wall. In two patients, bladder wall involvement was diagnosed with MR imaging, whereas the lesion was limited to the peritoneum of the vesicouterine pouch at surgery. The sensitivity, specificity, positive and negative predictive values, and accuracy of MR imaging for the diagnosis of bladder involvement were 88% (14 of 16), 98.9% (177 of 179), 88% (14 of 16), 98.9% (177 of 179), and 97.9% (191 of 195), respectively.

Frozen pelvis.—In 15 patients, involvement of the structures of the posterior pelvic space (torus uterinus, USL, vagina, rectal wall) and adhesions to the posterior wall of the uterus that sometimes extended to the myometrium created a block of tissue that completely masked the pouch of Douglas (Fig 7). In some of these patients, the fibrosis encased the pelvic ureter. Some of these patients also had huge lesions of endometriosis in the anterior pelvic space, and these lesions formed a block of tissue between the bladder and the uterus.

In all these patients, the diagnosis of endometriosis at MR imaging was determined preoperatively on the basis of the association with morphologic findings, signal intensity characteristics, and usual characteristic pathways of endometriosis (21). Endometriosis was confirmed at surgery. No carcinoma was diagnosed at pathologic examination.

Associated Lesions of Endometriosis

MR imaging yielded a diagnosis of endometriomas in 120 patients. Two patients had false-negative results and 11 had false-positive results. The sensitivity,

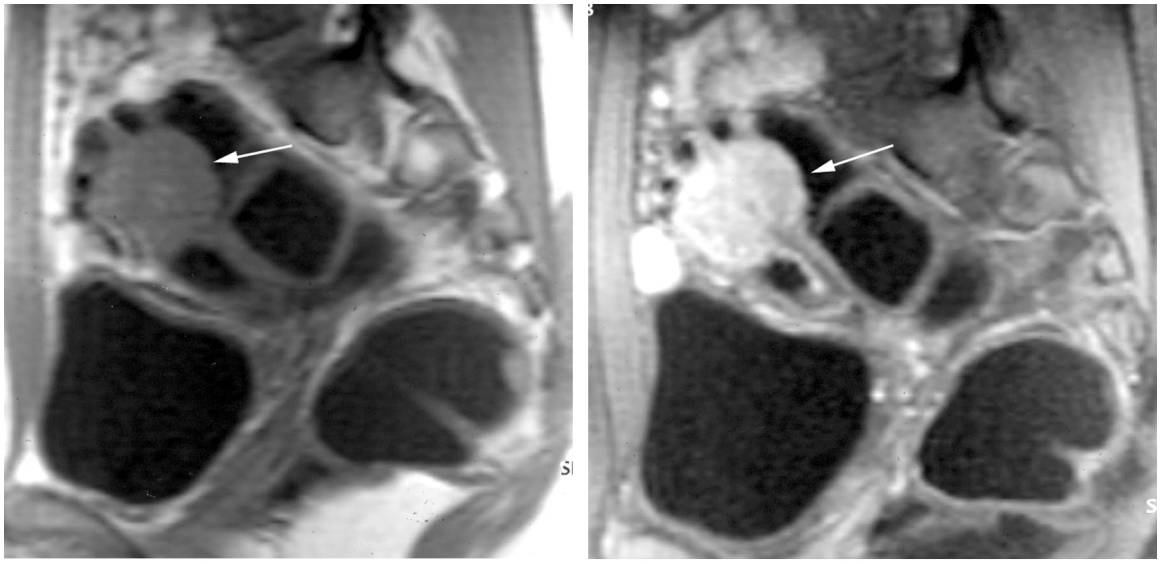

a. **b.**

Figure 5. Sagittal T1-weighted fast low-angle shot MR image (100/13; flip angle, 65°) obtained after rectal enema **(a)** before and **(b)** after intravenous injection of gadolinium-based contrast material demonstrates large fibrotic nodule (arrow) in inferior part of sigmoid colon. True-positive diagnosis of sigmoid colon involvement with endometriosis was determined at MR imaging.

specificity, and positive and negative predictive values of MR imaging for the diagnosis of endometriomas were 98.2% (109 of 111), 87% (73 of 84), 90.8% (109 of 120), and 97% (73 of 75), respectively. The accuracy of MR imaging was 93.3% (182 of 195).

MR imaging yielded a diagnosis of superficial peritoneal endometriosis in 13 patients. Seventy-five patients had false-negative results, and seven had false-positive results. The sensitivity, specificity, and positive and negative predictive values of MR imaging for the diagnosis of superficial peritoneal endometriosis were 5% (four of 81), 93.9% (107 of 114), 36% (four of 11), and 58.2% (107 of 184), respectively. The accuracy of MR imaging was 56.9% (111 of 195).

In 163 patients with pelvic endometriosis, the uterus was anteflexed in 115 (70.6%), retroflexed in 46 (28.2%), or absent in two (1.2%). In 97 patients with deep pelvic posterior endometriosis, the uterus was anteflexed in 66 (68%), retroflexed in 29 (30%), or absent in two (2%). Endometriosis was suggested at MR imaging in 44 patients and was confirmed at hysterectomy in seven patients.

TABLE 9
Intestinal Involvement: Correlation between MR Imaging Results and Pathologic Findings

MR Imaging Results	Positive Pathologic Findings	Negative Pathologic Findings	No. of Patients
Positive	37	0	37
Negative	2	156	158
Total	39	156	195

Note.—Positive indicates that intestinal involvement was present, and negative indicates that it was not. Sensitivity was 95%; specificity, 100%; positive predictive value, 100%; negative predictive value, 98.7%; and accuracy, 99.0%.

DISCUSSION

We believe ours is the first diagnostic MR imaging study of locations of deep pelvic endometriosis in a large series of patients. Overall, we obtained a sensitivity of 90.3%, a specificity of 91%, a positive predictive value of 92.1%, a negative predictive value of 89%, and an accuracy of 90.8%.

A variety of techniques (transvaginal sonography, transrectal sonography, and endoscopic transrectal sonography) have been used to diagnose deep pelvic endometriosis and to assess its extension in specific locations such as the bladder, the USL, the rectovaginal septum, and the rectal wall, with varying results (7,8,22,23). Although transrectal sonography has been reported to have a sensitivity of 80% and a specificity of 97% for the diagnosis of USL involvement (22), no large studies of a comparison of sonography and MR imaging have been published. Endoscopic transrectal sonography has been reported to be useful for the diagnosis of rectal wall endometriosis, with a sensitivity and specificity of 100% (8,23,24). Bazot et al (25), however, demonstrated that transvaginal sonography was as efficient as endoscopic transrectal sonography for the diagnosis and evaluation of extension of rectal endometriosis. In contrast to MR imaging, which offers an overview of the potential locations of pelvic endometriosis, the main limitation of the sonographic techniques is that they focus on a limited anatomic area of the pelvic cavity and subperitoneal space; none is individually capable of evaluation of overall pelvic extension.

As reported by Sampson (21), we found that the torus uterinus and the USL were the anatomic structures most frequently involved with deep pelvic endometriosis. Our data are in agreement with the frequency reported by several authors (26,27). Our results, however, differ from

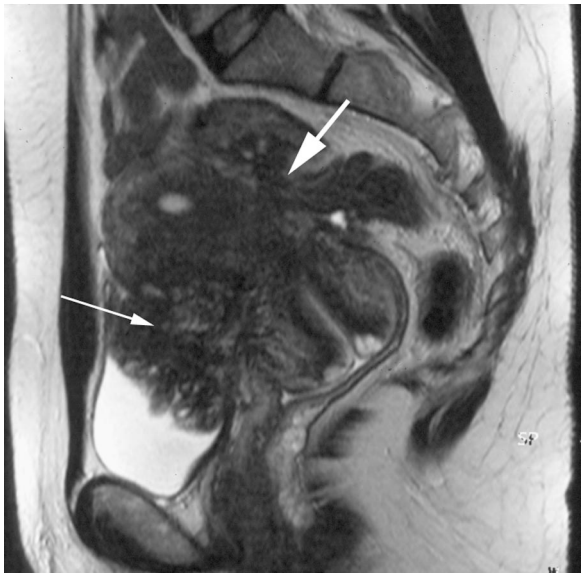

Figure 6. Sagittal T2-weighted fast spin-echo MR image (4,500/128) demonstrates large fibrotic area that protrudes into lumen, related to invasion of mucosal layer, and that forms a vesicouterine block of tissue with associated diffuse anterior endometriosis (thin arrow). Complete obstruction of vesicouterine pouch and rectal wall involvement (thick arrow) are present. True-positive diagnosis of bladder endometriosis was determined at MR imaging.

Figure 7. Sagittal T2-weighted fast spin-echo MR image (4,500/128) demonstrates typical fibromuscular lesions of endometriosis (arrow) that contain hyperintense foci in intestinal wall and extend into posterior wall of uterus. High degree of extension and adhesions at preoperative evaluation suggest difficulty of resection. At surgery, frozen pelvis was confirmed; at biopsy, endometriosis was diagnosed. True-positive diagnosis of intestinal endometriosis was determined at MR imaging.

TABLE 10
Bladder Involvement: Correlation between MR Imaging Results and Surgical and Pathologic Findings

MR Imaging Results	Positive Surgical and Pathologic Findings	Negative Surgical and Pathologic Findings	No. of Patients
Positive	14	2	16
Negative	2	177	179
Total	16	179	195

Note.—Positive indicates that bladder involvement was present, and negative indicates that it was not. Sensitivity was 88%; specificity, 98.9%; positive predictive value, 88%; negative predictive value, 98.9%; and accuracy, 97.9%.

those of Kinkel et al (13), who observed USL involvement in 100% of patients. Although Kinkel et al used a USL thickness of greater than 9 mm to define involvement of the ligament, we found that localized thickening of less than 9 mm, asymmetry between the two ligaments, and their irregularity were more specific than simply a thickness measurement. The diagnosis of endometriosis of the USL is simple when both ligaments are involved together with the torus uterinus. With this involvement, a typical arciform pattern or an irregular unilateral thickening, a nodule, or a stellate pattern is formed, particularly when hemorrhagic implants or associated rectal involvement are present. In our series, the main sources of false-negative and false-positive results were a retroflexed uterus, an adhesion, and an endometrioma, which masked the insertion of and the proximal part of the USL.

With respect to surgical findings, we found that MR imaging had a sensitivity of 88.3%, a specificity of 97.8%, a positive predictive value of 95%, a negative predictive value of 95.0%, and an accuracy of 94.9% for intestinal involvement. In clinical practice, the most frequent location with the MR imaging pattern that was most characteristic of endometriosis was the rectosigmoid junction. This location, which was always associated with torus uterinus involvement in our series, was usually visualized as an anterior displacement of the rectum (which appeared to be attracted toward the torus uterinus), as thickening of the anterior rectal wall with formation of an obtuse angle with the normal wall, and sometimes as an area that contained hyperintense foci on T2-weighted MR images or on T1-weighted MR images obtained with or without fat suppression, with better delineation after contrast enhancement. In more extensive cases, complete adhesions (3–8 cm) were found between the anterior wall of the rectum and the posterior wall of the uterus and were associated with typical aspects of endometriosis, as reported by Sampson (21).

When endometriosis of the torus uterinus and the USL is juxtaposed to the rectal wall, involvement limited to the serosa or with invasion of the muscle wall can be difficult to diagnose. In seven of our patients, this extension was wrongly diagnosed (ie, not confirmed with surgical findings) and was correctly

diagnosed in only two patients. These results underline the difficulty in the differentiation of lesions that are limited to the serosa from lesions that invade the muscle wall. Conversely, three positive diagnoses at MR imaging that were based on the criteria described in Materials and Methods were not confirmed at surgery in our series. In one of the patients, a limited nodule on the inferior face of the sigmoid colon was not found by the surgeon, whereas in the other two patients, extensive adhesions were the most likely explanation for the false-positive MR imaging results.

When deep pelvic endometriosis is located in the sigmoid colon, it can be missed at MR imaging or be confused with fecal material. A water enema administered prior to MR imaging is very helpful for the diagnosis at this site of involvement, as previously reported by Kinkel et al (13). When the lesion is located in the rectum at the level of the lower cervix or the rectovaginal septum, the MR imaging pattern is usually very characteristic. The main problem in this location is to define downward extension, which may or may not involve the rectovaginal septum. These locations are most commonly associated with upward attraction of the vaginal fornix, and this attraction hinders the diagnosis of rectovaginal septum involvement both before and at surgery.

During embryogenesis, the rectovaginal septum arises from the fusion of the two leaves of the peritoneal cul-de-sac and extends downward between the rectum and the vaginal wall to the level of the levator ani muscle (28). It is logical to think that endometriosis of the rectovaginal septum is, in most cases, secondary to involvement of the peritoneum of the pouch of Douglas, which is in direct juxtaposition to the top of the rectovaginal septum (29). Some rare locations have been reported as primary sites of endometriosis of the rectovaginal septum (30). In our series, all locations involved the pouch of Douglas and at least the upper third of the rectovaginal septum. The most characteristic MR imaging finding was involvement of the posterior wall of the vagina, and the anterior and lateral rectal walls showed irregular thickening with low signal intensity.

Vaginal involvement with endometriosis was almost always associated with obliteration of the pouch of Douglas. Comparisons of MR imaging results with surgical findings and with pathologic findings produced very high negative predictive values of 97.1% and 98.2%, respectively. Conversely, we obtained low positive predictive values of 67% and 50% for comparison of MR imaging results with surgical and pathologic findings, respectively. The main factor responsible for these false-positive results was extensive involvement of this space with endometriosis, with the usual difficulties of resection (frozen pelvis) and of determination of the anatomic site of tissue sampling.

Bladder endometriosis was present in 16 (15.5%) of 103 patients and was isolated in only six (5.8%) patients. In all but one patient, it was located in the dome of the bladder in front of the vesicouterine pouch (7,13). The most characteristic finding was a 2–4-cm mass that formed an obtuse angle with the bladder wall and that was mainly hypointense and almost always contained hyperintense foci on T1- and T2-weighted MR images and fat-suppressed T1-weighted MR images. Endometrial lesions of the anterior wall of the uterus were sometimes associated with these findings (7,31). Although endometriosis in this space is usually easy to diagnose, it can be difficult to accurately locate lesions in the vesicouterine pouch alone or lesions that extend into the bladder wall, as in the two patients with false-negative results and in the two patients with false-positive results in our series. The main limitation of MR imaging in the preoperative evaluation of this lesion is in the definition of the precise anatomic relationship of the bladder involvement with the ureteral meatus.

MR imaging has the advantages of aiding in the detection of all deep pelvic sites of endometriosis and of providing accurate depiction of extension of the disease for the surgeon. Preoperative diagnosis of extensive cases can provide a warning to the surgeon that dissection may be particularly difficult. In case of severe infiltration with complete obliteration of the pouch of Douglas (20), MR imaging, with its high contrast resolution and multiplanar imaging capacity, can help in the analysis of lesions that are difficult or impossible to explore during surgery. Moreover, as previously suggested by Siegelman et al (18), MR imaging could help in the differentiation of deep pelvic endometriosis from malignant carcinomatosis.

The diagnosis of deep pelvic endometriosis was confirmed histologically in 63.2% of patients. This low rate could be explained by the strict histologic criteria we used that were based on the presence of both endometrial glandular and stromal tissue. As previously demonstrated, however, the glandular component found in deep lesions is relatively small, and serial sectioning is required to confirm the diagnosis of endometriosis (25,32). Although histologic examination remains the standard for the diagnosis of endometriosis, some lesions diagnosed at surgery are not examined at biopsy, as their pattern with direct visualization is sufficiently characteristic (19). Some deep lesions typical of endometriosis on MR images are not visualized during surgery because they are hidden by adhesions or enclosed in a block of tissue.

Several limitations of our study must be considered. First, the prevalence of pelvic endometriosis and specifically of deep pelvic endometriosis was particularly high in the study, and this prevalence represents a possible source of bias. Second, some artifacts may alter the interpretation of MR imaging results; these include artifacts from peristalsis, a rectum filled with fecal materials, an empty bladder, and the morphologic characteristics of some patients. Finally, results of the examinations were interpreted by only two radiologists who were experienced in the field of gynecologic imaging. This limitation causes one to recall the results of a previous study (33) in which the researchers demonstrated that the accuracy of MR imaging depended on MR imaging sequences, artifacts, and the experience of radiologists in the field of gynecologic imaging.

In conclusion, MR imaging demonstrates high sensitivity, specificity, positive and negative predictive values, and accuracy in the prediction of the locations of extension of disease in patients with deep pelvic endometriosis.

Acknowledgment: We thank Pierre P. Lévy, MD, Unité de biostatistique et informatique médicale, Hôpital Tenon, Assistance Publique-Hopitaux de Paris, France, for statistical revision.

References

1. Clement MD. Diseases of the peritoneum (including endometriosis). In: Kurman RJ, ed. Blaustein's pathology of the female genital tract. 5th ed. New York: Springer-Verlag, 2002; 729–789.
2. Testut L. Traité d'anatomie topographique avec applications médico-chirurgicales. In: Latarjet A, ed. Traité d'anatomie humaine. Paris, France: Doin, 1931.
3. Cornillie FJ, Oosterlynck D, Lauweryns JM, et al. Deeply infiltrating pelvic endometriosis: histology and clinical significance. Fertil Steril 1990; 53:978–983.
4. Koninckx PR, Martin D. Treatment of deeply infiltrating endometriosis. Curr Opin Obstet Gynecol 1994; 6:231–241.
5. Mais V, Guerriero S, Ajossa S, et al. The

efficiency of transvaginal ultrasonography in the diagnosis of endometrioma. Fertil Steril 1993; 60:776–780.
6. Guerriero S, Mais V, Ajossa S, et al. The role of endovaginal ultrasound in differentiating endometriomas from other ovarian cysts. Clin Exp Obstet Gynecol 1995; 22:20–22.
7. Fedele L, Bianchi S, Raffaelli R, et al. Preoperative assessment of bladder endometriosis. Hum Reprod 1997; 12:2519–2522.
8. Roseau G, Dumontier I, Palazzo L, et al. Rectosigmoid endometriosis: endoscopic ultrasound features and clinical implications. Endoscopy 2000; 32:525–530.
9. Chapron C, Dubuisson JB. Management of deep endometriosis. Ann N Y Acad Sci 2001; 943:276–280.
10. Zawin M, McCarthy S, Scoutt L, et al. Endometriosis: appearance and detection at MR imaging. Radiology 1989; 171:693–696.
11. Togashi K, Nishimura K, Kimura I, et al. Endometrial cysts: diagnosis with MR imaging. Radiology 1991; 180:73–78.
12. Balleyguier C, Chapron C, Dubuisson JB, et al. Comparison of magnetic resonance imaging and transvaginal ultrasonography in diagnosing bladder endometriosis. J Am Assoc Gynecol Laparosc 2002; 9:15–23.
13. Kinkel K, Chapron C, Balleyguier C, et al. Magnetic resonance imaging characteristics of deep endometriosis. Hum Reprod 1999; 14:1080–1086.
14. Nishimura K, Togashi K, Itoh K, et al. Endometrial cysts of the ovary: MR imaging. Radiology 1987; 162:315–318.
15. Ha HK, Lim YT, Kim HS, et al. Diagnosis of pelvic endometriosis: fat-suppressed T1-weighted vs conventional MR images. AJR Am J Roentgenol 1994; 163:127–131.
16. Togashi K, Nishimura K, Itoh K, et al. Adenomyosis: diagnosis with MR imaging. Radiology 1988; 166:111–114.
17. Bazot M, Cortez A, Darai E, et al. Ultrasonography compared with magnetic resonance imaging for the diagnosis of adenomyosis: correlation with histopathology. Hum Reprod 2001; 16:2427–2433.
18. Siegelman ES, Outwater E, Wang T, et al. Solid pelvic masses caused by endometriosis: MR imaging features. AJR Am J Roentgenol 1994; 163:357–361.
19. Adamson GD, Nelson HP. Surgical treatment of endometriosis. Obstet Gynecol Clin North Am 1997; 24:375–409.
20. Reich H, McGlynn F, Salvat J. Laparoscopic treatment of cul-de-sac obliteration secondary to retrocervical deep fibrotic endometriosis. J Reprod Med 1991; 36:516–522.
21. Sampson JA. Perforating hemorrhagic (chocolate) cysts of the ovary: their importance and especially their relation to pelvic adenomas of endometrial type ("adenomyoma of the uterus, rectovaginal septum, sigmoid, etc"). Arch Surg 1921; 3:245–323.
22. Fedele L, Bianchi S, Portuese A, et al. Transrectal ultrasonography in the assessment of rectovaginal endometriosis. Obstet Gynecol 1998; 91:444–448.
23. Chapron C, Dumontier I, Dousset B, et al. Results and role of rectal endoscopic ultrasonography for patients with deep pelvic endometriosis. Hum Reprod 1998; 13:2266–2270.
24. Dumontier I, Roseau G, Vincent B, et al. Comparison of endoscopic ultrasound and magnetic resonance imaging in severe pelvic endometriosis. Gastroenterol Clin Biol 2000; 24:1197–1204.
25. Bazot M, Detchev R, Cortez A, et al. Transvaginal sonography and rectal endoscopic sonography for the assessment of pelvic endometriosis: a preliminary comparison. Hum Reprod 2003; 18:1686–1692.
26. Redwine DB. The distribution of endometriosis in the pelvis by age groups and fertility. Fertil Steril 1987; 47:173–175.
27. Chapron C, Fauconnier A, Vieira M, et al. Anatomical distribution of deeply infiltrating endometriosis: surgical implications and proposition for a classification. Hum Reprod 2003; 18:157–161.
28. Uhlenhuth E, Wolfe WM, Middleton EB. The rectogenital septum. Surg Gynecol Obstet 1948; 76:148–163.
29. Chapron C, Liaras E, Fayet P, et al. Magnetic resonance imaging and endometriosis: deeply infiltrating endometriosis does not originate from the rectovaginal septum. Gynecol Obstet Invest 2002; 53:204–208.
30. Nisolle M, Donnez J. Peritoneal endometriosis, ovarian endometriosis, and adenomyotic nodules of the rectovaginal septum are three different entities. Fertil Steril 1997; 68:585–596.
31. Fedele L, Piazzola E, Raffaelli R, et al. Bladder endometriosis: deep infiltrating endometriosis or adenomyosis? Fertil Steril 1998; 69:972–975.
32. Anaf V, Simon P, Fayt I, et al. Smooth muscles are frequent components of endometriotic lesions. Hum Reprod 2000; 15:767–771.
33. Bazot M, Darai E, Clément de Givry S, et al. Fast breath-hold T2-weighted MR imaging reduces interobserver variability in the diagnosis of adenomyosis. AJR Am J Roentgenol 2003; 180:1291–1296.